minerals

Characterization of Bentonites from the *in situ* ABM5 Heater Experiment at Äspö Hard Rock Laboratory, Sweden

Ana María Fernández [1,*], José F. Marco [2], Paula Nieto [1], Fco. Javier León [1], Luz María Robredo [1], María Ángeles Clavero [1], Ana Isabel Cardona [1], Sergio Fernández [1], Daniel Svensson [3] and Patrik Sellin [3]

[1] CIEMAT, Centro de Investigaciones Energéticas, Medioambientales y Tecnológicas, Departamento de Medio Ambiente, 28040 Madrid, Spain; paul.nch@gmail.com (P.N.); fcojavier.leon@ciemat.es (F.J.L.); l.robredo@ciemat.es (L.M.R.); ma.clavero@ciemat.es (M.Á.C.); anaisabel.cardona@ciemat.es (A.I.C.); sergio.fernandez@ciemat.es (S.F.)

[2] CSIC, Consejo Superior de Investigaciones Científicas, Instituto de Química Física "Rocasolano", 28006 Madrid, Spain; jfmarco@iqfr.csic.es

[3] Department of Research and Safety Assessment, SKB—Svensk Kärnbränslehantering, SE-57229 Oskarshamn, Sweden; daniel.svensson@skb.se (D.S.); patrik.sellin@skb.se (P.S.)

* Correspondence: anamaria.fernandez@ciemat.es

Materials

MX-80 bentonite, a type of Wyoming bentonite coming from USA. This bentonite is composed by a sodium montmorillonite (~82-84 wt.%) that occurs as layers in marine shales, and is widespread and extensively mined, not only in Wyoming but also in parts of Montana and South Dakota. The bentonite formed through alteration of rhyolitic tephra deposited in ancient Mowry Sea basin during the Cretaceous, more than 65 million years ago [1].

IBECO Deponit-CA-N is a Greek bentonite, quarried by S&B Industrial Minerals, S.A. in the north-eastern part of the island of Milos. Pyroclastic tuffs and lavas of andesitic to dacitic composition are the main parent rocks of this bentonite, which forms irregular bodies with a thickness of 10–40 m within the pyroclastics. The bentonite formation is a result of hydrothermal reactions between the permeable volcanic rocks and percolating groundwater heated to below 90°C during volcanic activity, although there is some disagreement about the genesis, e.g. [2]. The major mineral phase (80-84 wt.%) is calcium montmorillonite.

Rokle bentonite originates from the Rokle deposit in the Kadan basin within the north Bohemian volcanic areas c. 100 km WNW of Prague (Czech Republic). The deposit is part of a series of argillised volcanoclastic accumulations of Tertiary age, formed by auto-hydrothermal alteration in shallow lacustrine basins within the stratovolcano complex of Doupovské Mountains. The bentonite is capped by basaltic lava-flows. The lens-shaped bentonite body has a maximum thickness of c. 40 m and contains more than 40 million tons of bentonite. The volcanic glass is completely altered to smectite, but mm-sized flakes of biotite, which is a primary constituent of the basaltic magma, are relatively frequent. The bentonite is highly variable in colour, ranging from olive-grey to yellow/red due to the admixture of secondary iron and manganese oxides [3,4]. The major mineral phase (~70 wt.%) is calcium montmorillonite, containing also some kaolinite.

FEBEX bentonite was extracted from the Cortijo de Archidona deposit (Serrata de Níjar, Almería, Spain). In this zone, the bentonite deposits are usually associated with fractures, the origin being related to hydrothermal alteration processes that took place in tuffaceous volcanic rocks 15-5 Ma ago (Miocene age). The major mineral phase (90-92 %) is a Ca-Mg-montmorillonite, predominantly calcium [5,6].

Asha 505 is the commercial name of extensive deposits of natural Na-bentonite quarried in the Kutch area, 60-80 Km from the ports of Kandla and Mandvi on the north-west-coast of India. The bentonite is associated with the basaltic Deccan Trap rocks of Tertiary age and formed through hydrothermal alteration of volcanic ash in saline water [7]. The bentonite occurs in scattered pockets or layers within the basaltic rocks, with thicknesses ranging between few to 30 meters. The major mineral phase (80-87 wt.%) is sodium montmorillonite, also containing some kaolinite. Because of the high content of secondary iron oxides, the color is normally dark reddish brown.

Table S1. Mineral phases observed in the bentonite samples by means of XRD, FTIR and SEM techniques.

Type of mineral phases	Mineral phases	Original Samples	Granite contact	Medium part	Heater contact
Fe-oxyhydroxides	Goethite (weak FM) (Gth)	Asha 505 Rokle	Asha B28 Rokle B14	Asha B28 Febex B25 Rokle B14 MX-80 B1	Asha B28 Febex B25 Rokle B14 MX-80 B1
	Hematite (AFM) (Hem)	Asha 505 MX-80	Asha B28 MX-80 B1	Asha B28 MX-80 B1	Asha B28 Rokle B14 MX-80 B1
	Magnetite (FM) (Mag)	NO	NO	NO	NO
	Titanomagnetite (Tmag)	NO	NO	NO	NO
	Maghemite (FM) (Mgh)	NO	NO	NO	NO
	Ferrihydrite (Fhy)	NO	NO	NO	NO
Carbonates	Calcite (Cal)	All	All	All	All
	Monohydrocalcite (MhCal)	NO	NO	NO	MX-80 B1
	Dolomite (Dol)	Rokle	Rokle B14	Rokle B14	Rokle B14
	Magnesite (Mgs)	NO	NO	NO	NO
	Siderite (Sd)	Rokle MX-80	Rokle B14 MX-80 B1	Febex B25 Rokle B14 MX-80 B1	Febex B25 Rokle B14 MX-80 B1
Sulfides	Pyrrhotite (Pyh)	NO	NO	NO	NO
	Mackinawite (Mkw)	NO	NO	NO	NO
	Pyrite (Py)	MX-80	MX-80 B1	Asha B28 Rokle B14 MX-80 B1	Asha B28 Rokle B14 MX-80 B1
	Sphalerite (Sp)	NO	NO	NO	MX-80 B1
Sulfates	Gypsum (Gp)	MX-80	MX-80 B1	Asha B28 MX-80 B1	Asha B28 MX-80 B1
	Barite (Ba)	?	?	?	Febex B25 Rokle B14
Silica oxides	Quartz (Qz)	All	All	All	All
	Cristobalite (Crs)	All	All	All	All
	Tridymite (Trd)	?	?	?	Rokle B14
Feldspars	K-felspars (KFs)	All	All	All	All
	Plagioclases (Pl)	All	All	All	All
Titanium oxides	Anatase (Ant)	Rokle	Rokle B14	Asha B28 Rokle B14	Rokle B14
Mg-hydroxides	Brucite (Brc)	No	No	No	No
Zeolites	Clinoptilolite (Cpt)	No	No	Asha B28	Asha B28
Smectites	Montmorillonite (Mnt)	All	All	All	All
	Saponite (Sap)	No	No	No	No
Illite/Muscovite	Illite (Ilt)/Muscovite (Ms)	Febex B25 Rokle MX-80	Febex B25 Rokle B14 MX-80 B1	Febex B25 Rokle B14 MX-80 B1	Febex B25 Rokle B14 MX-80 B1
Kaolinites	Kaolinite (Kln)	Asha 505 Rokle	Asha B28 Rokle B14	Asha B28 Rokle B14	Asha B28 Rokle B14

Chlorites	Clinochlore(Clc)/ Chamosite (Chm)	No	No	No	No

Table S2. Positions and assignments of vibrational bands of dioctahedral smectites, kaolinite and illite.

Wavenumber (cm^{-1})	Assignment [8–11]
3800-3500	OH stretching of inner structural hydroxyl groups (influenced by nature of the coordinated octahedral cations): - AlAlOH (dioctahedral): 3623 cm^{-1} - Mg_3OH (trioctahedral): 3680 cm^{-1} - FeFeOH: 3567 cm^{-1}
3426	OH stretching of adsorbed water
3240	OH stretching of adsorbed water
3150-3170	Fe-oxyhydroxide
1634	OH bending of adsorbed water
1430 (872, 712)	ν_{3g}-CO_3 asymmetric stretching of calcite (ν_2: out of plane bending, ν_4: planar bending): calcite
1115	Si-O stretching vibration (out-of-plane)
1030-1020	Si-O stretching vibration (in-plane): - Dioctahedral: 1030 cm^{-1} - Trioctahedral: 1020 cm^{-1}
917	Kaolinite inner OH deformation
915	AlAlOH bending
885	AlFeOH bending
850	AlMgOH bending
820	FeFeOH bending (nontronite: 817, 676 cm^{-1})
795	MgMgOH bending
765	FeMgOH bending
792	Kaolinite Si-O-Al vibrations
792 790/800 798 & 780 doublet 794	Si-O stretching of silica Amorphous silica (opal, volcanic glass, etc.) Quartz Cristobalite
754	Kaolinite Si-O-Al vibrations
750	Illite Al-O-Si vibration
700	Illite OH bending
698	Kaolinite OH translation
655-660	Mg3OH bending (saponite)
644	Kaolinite inner surface OH vibration
626 792, 624 790	Coupled Al-O and Si-O (out-of-plane), Si-O of cristobalite Si-O of tridymite
624	R-O-Si with R=Al, Mg, Fe
539	Kaolinite Si-O-Al (out of plane) bending (Al in tetrahedral sheet)
520	Si-O-Al bending (Al tetrahedral cation)
465	Si-O-Si bending vibration
426	Si-O bending vibration
825, 750	Illite
740, 790, 890, 1150	Fe oxyhydroxide
Complex bands 400-900	Feldspars

Table S3. Chemical composition of the solid phase (total fraction) for different samples obtained after dismantling of ABM5 experiment: Asha Block 28, Febex Block 25 and Rokle Block 11.

Samples	**Asha Block 28**				**FEBEX Block 25**				**Rokle Block 11**			
/ wt.%	**Ref.[12]**	**G**	**H**	**M**	**Ref.**	**G**	**M**	**H**	**Ref.**	**G**	**M**	**H**
Distance to Heater (cm)	10	8.3	5.0	1.7	10	8.3	5.0	1.7	10	8.3	5.0	1.7
SiO_2	46.48	45.53	44.56	45.51	55.46	61.48	61.04	60.57	48.06	43.62	44.02	42.98
Al_2O_3	20.64	19.44	18.94	19.34	17.28	18.02	17.98	18.09	14.52	14.15	14.16	14.14
Fe_2O_3	12.16	23.34	24.05	21.87	3.09	6.64	6.60	8.16	15.94	24.04	23.75	24.62
MgO	2.01	2.60	2.60	2.60	4.37	4.10	4.20	4.10	2.12	2.50	2.40	2.50
CaO	0.84	3.23	3.55	3.87	1.75	4.02	3.89	3.32	2.85	3.45	3.45	3.31
Na_2O	1.97	1.60	1.60	1.60	1.16	1.40	1.90	1.30	0.26	1.30	1.50	1.60
K_2O	0.14	0.39	0.38	0.43	0.99	1.77	1.79	1.76	1.00	1.50	1.47	1.48
SrO	0.02	0.04	0.04	0.03	0.02	0.05	0.06	0.07	0.04	0.08	0.08	0.08
TiO_2	1.01	1.74	1.51	1.68	0.15	0.23	0.30	0.31	4.51	6.61	6.50	6.58
P_2O_5	0.09	< d.l.	0.16	0.16	0.03	< d.l.	0.10	0.11	0.84	0.71	0.67	0.65
MnO	0.05	0.08	0.06	0.07	0.03	0.04	0.04	0.03	0.19	0.09	0.09	0.08
ZnO	0.02	0.05	0.04	0.05	0.01	0.02	0.02	0.02	0.02	0.03	0.03	0.03
Cr_2O_3	0.04	0.13	0.11	0.13	< d.l.	0.02	0.02	< d.l.	0.03	0.00	0.08	0.09
CuO	0.02	0.04	0.03	0.03	< d.l.	< d.l.	< d.l.	< d.l.	0.03	0.04	0.04	0.04
NiO	0.01	0.02	0.02	0.03	< d.l.	0.01	< d.l.	< d.l.	0.01	0.01	< d.l.	< d.l.
ZrO_2	0.01	0.02	0.02	0.01	0.02	0.03	0.04	0.05	0.06	0.10	0.10	0.11
SnO_2	< d.l.	0.01	0.01	0.01	< d.l.	< d.l.	< d.l.	< d.l.	< d.l.	< d.l.	< d.l.	0.01
CdO	< d.l.	< d.l.	0.01	0.01	< d.l.	< d.l.	< d.l.	< d.l.	< d.l.	< d.l.	< d.l.	< d.l.
V_2O_5	0.07	0.04	< d.l.	< d.l.	0.01	< d.l.	< d.l.	0.01	< d.l.	< d.l.	< d.l.	< d.l.
PbO	< d.l.	< d.l.	< d.l.	< d.l.	< d.l.	0.02	0.02	0.02	< d.l.	< d.l.	< d.l.	< d.l.
SO_3	0.15	0.58	1.12	1.42	< d.l.	0.59	0.59	0.64	0.05	0.57	0.55	0.61
Cl	0. 30	1.16	1.19	1.10	0.024	1.58	1.45	1.40	0.002	1.19	1.08	1.02

Table S4. Chemical composition of the solid phase (total fraction) for different samples obtained after dismantling of ABM5 experiment: IBECO Block 11, MX-80 Block 1.

Samples	**IBECO Block 11**				**MX-80 Block 1**		
/ wt.%	**Ref.**	**G**	**3**	**2**	**Ref.**	**G**	**M**
Distance to Heater (cm)	10	8.75	6.25	3.75	10	8.3	5.0
SiO_2	50.32	60.34	60.36	60.90	62.89	60.64	60.15
Al_2O_3	15.7	17.71	18.63	18.41	19.87	20.03	20.01
Fe_2O_3	4.76	6.52	6.71	6.94	3.53	7.60	7.50
MgO	4.76	5.30	4.60	4.40	2.40	2.70	2.70
CaO	5.29	3.47	3.52	3.69	1.24	4.22	4.23
Na_2O	0.89	2.40	2.10	1.60	2.09	1.60	1.70
K_2O	0.55	1.23	1.29	1.24	0.52	0.91	0.87
SrO	0.02	0.05	0.06	0.06	0.03	0.08	0.08
TiO_2	0.63	0.60	0.61	0.55	0.07	< d.l.	0.21
P_2O_5	0.11	0.07	< d.l.	0.14	0.03	< d.l.	0.15
MnO	0.12	0.08	0.06	0.06	0.01	0.05	0.03
ZnO	0.01	0.03	0.03	0.02	0.01	0.02	0.02
ZrO_2	0.02	0.03	0.04	0.04	0.03	0.04	0.04
PbO	0.00	0.01	< d.l.	< d.l.	0.00	0.02	0.02
SO_3	0.19	0.63	0.59	0.66	0.19	1.18	1.40
Cl	0.009	1.41	1.34	1.29	0.003	0.85	0.81

Table S5. Fe(II), Fe(II) and total Fe contents obtained after dismantling of ABM5 experiment.

Samples	Distance to heater (cm)	Fe(II) wt.%	Total Fe wt.%	Fe(III) wt.%	Fe(II)/Fe(III)	Fe(II) in Total Fe wt.%
MX-80 Ref.	--	0.27	2.40	2.13	0.13	11.25
MX-80 B1 G	8.3	0.62	2.88	2.26	0.27	21.54
MX-80 B1 M	5.0	0.63	2.85	2.22	0.28	22.14
MX-80 B1 H	1.7	0.66	5.11	4.44	0.15	12.99
IBECO Ref.	--	0.19	3.10	2.91	0.07	6.13
IBECO B11 G	8.75	0.29	2.15	1.86	0.16	13.65
IBECO B11 3	6.25	0.30	2.19	1.89	0.16	13.57
IBECO B11 2	3.75	0.35	2.22	1.87	0.19	15.86
IBECO B11 H	1.25	0.60	3.36	2.76	0.22	17.81
Rokle Ref.1	--	0.37	6.97	6.60	0.06	5.28
Rokle B14 G	8.3	0.26	8.98	8.72	0.03	2.94
Rokle B14 M	5.0	0.30	8.96	8.66	0.03	3.31
Rokle B14 H	1.7	0.36	9.59	9.22	0.04	3.81
Febex Ref.	--	0.15	2.30	2.15	0.07	6.52
FEBEX 25 G	8.3	0.14	1.86	1.72	0.08	7.54
FEBEX B25 M	5.0	0.16	1.90	1.74	0.09	8.37
FEBEX B25 H	1.7	0.30	2.21	1.91	0.16	13.51
Asha B28 G	8.3	0.19	5.74	5.55	0.03	3.32
Asha B28 M	5.0	0.21	6.66	6.45	0.03	3.18
Asha B28 H	1.7	0.27	5.60	5.34	0.05	4.74

Table S6. Parameters deduced from the BET and *t*-plot treatment on the adsorption of N_2 at 77 K from samples obtained after dismantling of ABM5 experiment.

Sample	Distance to heater (cm)	C_{BET}	V_m[1] (cm³/g)	S_{BET} (m²/g)	S_{tot}[2] (m²/g)	V_{tot}[3] (cm³/g)	S_{micro}[4] (m2/g)	V_{micr}[5] (cm3/g)	$S_{ext\ micro}$[6] (m2/g)	$S_{ext\ meso}$[7] (m²/g)	V_{meso}[8] (cm³/g)
Asha B28 G	8.30	209.4	$2.31\cdot10^{-2}$ (l)	65.41	66.19	$1.06\cdot10^{-1}$	13.54	$5.28\cdot10^{-3}$	52.66	41.31	$1.15\cdot10^{-2}$ (l)
Asha B28 M	5.00	176.0	$1.98\cdot10^{-2}$ (l)	55.99	56.18	$1.02\cdot10^{-1}$	8.29	$3.29\cdot10^{-3}$	47.88	39.10	$7.99\cdot10^{-3}$ (l)
Asha B28 H	1.70	243.8	$2.18\cdot10^{-2}$ (l)	61.49	61.58	$1.08\cdot10^{-1}$	13.09	$5.50\cdot10^{-3}$	48.49	41.53	$9.39\cdot10^{-3}$ (l)
Febex B25 G	8.30	258.3	$1.35\cdot10^{-2}$ (l)	38.01	37.53	$7.80\cdot10^{-2}$	8.47	$3.78\cdot10^{-3}$	29.06	22.98	$7.03\cdot10^{-3}$ (l)
Febex B25 M	5.00	471.3	$1.62\cdot10^{-2}$ (l)	45.76	46.62	$8.90\cdot10^{-2}$	13.69	$5.59\cdot10^{-3}$	32.93	26.02	$9.28\cdot10^{-3}$ (l)
Febex B25 H	1.70	239.4	$1.28\cdot10^{-2}$ (l)	36.20	36.21	$8.41\cdot10^{-2}$	7.76	$3.27\cdot10^{-3}$	28.44	25.36	$4.99\cdot10^{-3}$ (l)
Rokle B14 G	8.30	341.8	$2.37\cdot10^{-2}$ (l)	66.90	67.32	$1.19\cdot10^{-1}$	17.53	$7.38\cdot10^{-3}$	49.78	38.76	$1.33\cdot10^{-2}$ (l)
Rokle B14 M	5.00	349.8	$2.27\cdot10^{-2}$ (l)	64.09	64.77	$1.15\cdot10^{-1}$	17.57	$7.27\cdot10^{-3}$	47.20	38.80	$1.18\cdot10^{-2}$ (l)
Rokle B14 H	1.70	287.8	$2.08\cdot10^{-2}$ (l)	58.70	59.39	$1.16\cdot10^{-1}$	14.42	$5.88\cdot10^{-3}$	44.94	41.01	$7.94\cdot10^{-3}$ (l)
IBECO B11 G	8.75	319.8	$1.76\cdot10^{-2}$ (l)	49.75	51.19	$9.77\cdot10^{-2}$	13.90	$5.35\cdot10^{-3}$	37.29	26.29	$1.14\cdot10^{-2}$ (l)
IBECO B11 3	6.25	403.4	$1.73\cdot10^{-2}$ (l)	48.98	50.76	$9.58\cdot10^{-2}$	16.28	$6.25\cdot10^{-3}$	34.49	25.75	$1.11\cdot10^{-2}$ (l)
IBECO B11 2	3.75	284.7	$1.59\cdot10^{-2}$ (l)	45.04	46.21	$9.06\cdot10^{-2}$	11.80	$4.54\cdot10^{-3}$	34.42	25.68	$9.42\cdot10^{-3}$ (l)
IBECO B11 H	1.25	400.8	$1.83\cdot10^{-2}$ (l)	51.71	53.88	$1.00\cdot10^{-1}$	16.52	$6.23\cdot10^{-3}$	37.36	27.55	$1.15\cdot10^{-2}$ (l)
MX 80 B1 G	8.30	436.5	$7.96\cdot10^{-3}$ (l)	22.48	23.45	$6.32\cdot10^{-2}$	6.94	$2.60\cdot10^{-3}$	16.52	14.45	$3.73\cdot10^{-3}$
MX 80 B1 M	5.00	188.7	$6.69\cdot10^{-3}$ (l)	18.91	19.19	$6.04\cdot10^{-3}$	3.17	$1.19\cdot10^{-3}$	16.02	14.91	$1.78\cdot10^{-3}$
MX 80 B1 H	1.70	256.9	$7.69\cdot10^{-3}$ (l)	21.72	22.33	$6.82\cdot10^{-2}$	4.74	$1.77\cdot10^{-3}$	17.60	16.05	$2.61\cdot10^{-3}$

[1]V_m: monolayer capacity derived from the BET treatment; expressed as (l): liquid; S_{BET}: BET Surface area.

[2]S_{tot}: Total surface area derived from the slope of the straight line passing through the origin of the *t*-plot.

[3]V_{tot}: Total pore volume, derived from the amount of nitrogen adsorbed at p/p_o of 0.98.

[4]S_{micro}:= S_{BET} – $S_{ext\ micro}$: Surface area of the micropores.

[5]V_{micr}: Liquid microporous volume derived from the ordinate at the origin in the second straight line of the *t*-plot.

[6]$S_{ext\ micro}$: Surface area derived from the slope of the second straight line of the *t*-plot.
[7]$S_{ext\ meso}$: Surface area derived from the slope of the third straight line of the *t*-plot.
[8]V_{meso}: Liquid microporous volume derived from the ordinate at the origin in the third straight line of the *t*-plot.

Table S7. Total cation exchange capacity (CEC) and cation exchange population prior and after dismantling of the ABM5 experiment (in meq/100g).

Sample	Distance to heater (cm)	Na	K	Mg	Ca	Sr	Ba	Σ CEC	CEC
Asha 505 Ref.	--	62.0	0.4	12.3	19.0	--	--	93.7	88.6
Asha B28 G	8.3	15.28	1.76	7.69	33.07	0.18	0.002	58.0	85.8
Asha B28 M	5.0	17.19	1.53	6.19	42.68	0.23	0.002	67.8	83.9
Asha B28 H	1.7	26.40	2.18	7.09	48.21	0.26	0.012	84.1	81.3
FEBEX Ref.	--	27.97	5.46	34.17	32.72	0.37	0.008	100.7	98.1
Febex B25 G	8.3	18.12	2.65	11.80	41.81	0.31	0.013	74.7	97.6
Febex B25 M	5.0	22.28	2.86	14.51	45.81	0.46	0.010	85.9	96.5
Febex B25 H	1.7	22.73	2.62	15.55	41.83	0.41	0.009	83.2	93.1
Rokle Ref.	--	0.61	4.72	19.08	52.48	0.14	0.010	77.1	73.8
Rokle B14 G	8.3	21.82	3.01	13.15	32.89	0.15	0.012	71.0	73.1
Rokle B14 M	5.0	23.06	3.02	11.42	30.94	0.14	0.012	68.6	73.0
Rokle B14 H	1.7	22.01	3.01	12.10	29.78	0.15	0.014	67.1	70.3
IBECO Ref.	--	25.19	4.31	31.37	34.67	0.20	0.019	95.8	90.2
IBECO B11 G	8.75	36.63	3.44	9.68	46.40	0.24	0.022	96.4	97.1
IBECO B11 3	6.25	37.64	3.15	9.31	46.32	0.24	0.019	96.7	97.9
IBECO B11 2	3.75	37.43	3.97	9.97	44.17	0.26	0.073	95.9	88.6
IBECO B11 H	1.25	34.38	3.16	8.95	43.94	0.23	0.017	90.7	95.0
MX-80 Ref.	--	58.49	4.18	6.86	15.63	0.44	0.009	85.6	83.6
MX-80 B1 G	8.3	23.95	1.31	8.78	48.42	0.53	0.008	83.0	84.1
MX-80 B1 M	5.0	23.45	1.32	8.80	47.15	0.53	0.006	81.2	87.6
MX-80 B1 H	1.7	24.52	1.40	12.65	46.31	0.55	0.007	85.4	87.8

Table S8. Soluble salts from aqueous leaching tests a 1:4 solid to liquid ration, in mg/L.

	Asha B28 G	Asha B28 M	Asha B28 H	Febex B25 G	Febex B25 M	Febex B25 H	Rokle B14 G	Rokle B14 M	Rokle B14 H	Ibeco B11 G	Ibeco B11 3	Ibeco B11 2	Ibeco B11 H	MX 80 B1 G	MX 80 B1 M	MX 80 B1 H
Distance to heater (cm)	8.30	5.00	1.70	8.30	5.00	1.70	8.30	5.00	1.70	8.75	6.25	3.75	1.25	8.30	5.00	1.70
w.c. (%)	16.8	17.6	13.4	13.8	13.3	13.2	8.6	8.9	8.1	13.6	13.1	13.6	13.6	11.6	11.6	11.4
Tot. mass (g)	5.02	5.00	5.01	5.00	5.00	5.01	5.00	5.00	5.01	5.04	5.00	2.50	5.01	5.00	5.01	5.00
Tot. water (g)	20.72	20.75	20.59	20.61	20.59	20.58	20.40	20.41	20.38	20.60	20.58	10.30	20.60	20.52	20.52	20.51
pH	7.8	7.6	7.8	7.7	7.8	7.7	7.8	8	7.9	7.8	7.8	7.7	7.9	7.7	7.5	7.6
Alk (meq/L)	1.23	0.77	1.5	0.86	1.18	0.87	1.38	1.74	1.76	1.10	1.22	1.40	1.25	1.17	1.06	1.03
F^-	1.1	0.52	0.15	1.1	1.2	1.3	1.6	1.7	1.7	1.1	0.94	1.1	0.8	1.2	0.86	0.98
Br^-	3.1	2.9	3	4.6	3.9	3.7	4.2	3.3	3	4.2	3.8	4.1	3.4	1.1	0.91	0.83
Cl^-	517	490	521	800	680	645	675	543	495	761	668	670	602	206	176	168
NO_3^-	<1.0	<1.0	<1.0	<1.0	<1.0	<1.0	<1	<1	<1	<1	<1	<1	<1	<1	<1	<1
SO_4^{2-}	155	937	742	147	182	114	151	144	128	103	95	99	100	635	930	939
Si	10	13	12	19	17	19	10	13	19	9.8	9.8	4.4	13	1.2	14	9.3
Na	420	650	630	570	510	470	520	450	420	550	500	500	470	440	500	500
K	5.1	9.3	9.3	11	11	11	18	17	16	14	13	14	13	12	14	15

Ca	13	78	61	23	18	13	15	11	8.8	13	10	11	9	29	54	53
Mg	1.4	6.5	8	4.5	4	3.5	4.2	3.2	2.6	1.8	1.4	1.5	1.2	3.3	5.9	5.9
Sr	0.13	0.67	0.56	0.32	0.34	0.25	0.17	0.14	0.11	0.16	0.13	0.14	0.11	0.71	1.4	1.5
Ba	<0.03	<0.03	<0.03	<0.03	<0.03	<0.03	0.07	0.06	0.05	0.05	0.04	0.04	0.03	0.04	0.05	0.06
B	0.66	1.1	1.4	0.53	0.8	0.31	0.09	0.05	<0.03	0.19	<0.22	<0.3	<0.16	<0.3	<0.3	<0.3
Fe	<0.03	<0.03	<0.03	<0.03	<0.03	<0.03	<0.03	<0.03	<0.03	<0.03	<0.03	<0.3	<0.03	<0.3	<0.3	<0.3
Mn	<0.03	<0.03	<0.03	<0.03	<0.03	<0.03	<0.03	0.04	0.04	<0.03	<0.03	<0.3	<0.03	<0.3	<0.3	<0.3
Al	<0.03	<0.03	<0.03	<0.03	<0.03	<0.03	0.03	<0.03	0.05	<0.03	<0.03	<0.3	<0.03	<0.3	<0.3	<0.3
Ti	<0.03	<0.03	<0.03	<0.03	<0.03	<0.03	<0.03	<0.03	<0.03	<0.03	<0.03	<0.3	<0.03	<0.3	<0.3	<0.3
Zn	<0.03	<0.03	<0.03	<0.03	<0.03	<0.03	<0.03	<0.03	<0.03	<0.03	<0.03	0.07	<0.03	0.22	<0.3	<0.3
Acetate	< 1	< 1	< 1	< 1	< 1	< 1	< 1	< 1	< 1	< 1	< 1	< 1	< 1	< 1	< 1	3.0
Formate	< 1	< 1	< 1	< 1	< 1	< 1	< 1	< 1	< 1	< 1	< 1	< 1	< 1	< 1	< 1	< 1

Table S9. Ion inventory obtained from aqueous leaching tests, in mol/100g.

Sample	Distance to heater (cm)	pH	Cl^-	F^-	Br^-	SO_4^{2-}	HCO_3^-
Asha B28 G	8.30	7.8	7.0309	0.0279	0.0187	0.7780	0.5928
Asha B28 M	5.00	7.6	6.7447	0.0134	0.0177	4.7601	0.3756
Asha B28 H	1.70	7.8	6.8495	0.0037	0.0175	3.6003	0.6989
Febex B25 G	8.30	7.7	10.5830	0.0272	0.0270	0.7177	0.4032
Febex B25 M	5.00	7.8	8.9476	0.0295	0.0228	0.8839	0.5503
Febex B25 H	1.70	7.7	8.4615	0.0318	0.0215	0.5520	0.4045
Rokle B14 G	8.30	7.8	8.4344	0.0373	0.0233	0.6964	0.6111
Rokle B14 M	5.00	8.0	6.8080	0.0398	0.0184	0.6663	0.7732
Rokle B14 H	1.70	7.9	6.1383	0.0393	0.0165	0.5858	0.7735
IBECO B11 G	8.75	7.8	9.9682	0.0269	0.0244	0.4979	0.5112
IBECO B11 3	6.25	7.8	8.7709	0.0230	0.0221	0.4604	0.5660
IBECO B11 2	3.75	7.9	7.9313	0.0197	0.0199	0.4863	0.6532
IBECO B11 H	1.25	7.7	8.8444	0.0271	0.0240	0.4823	0.5851
MX 80 B1 G	8.30	7.7	2.6612	0.0289	0.0063	3.0276	0.5372
MX 80 B1 M	5.00	7.5	2.2692	0.0207	0.0052	4.4255	0.4824
MX 80 B1 H	1.70	7.6	2.1656	0.0236	0.0047	4.4672	0.4706

Table S10. Calculated parameters and saturation indexes of the pore waters.

Sample	Asha Block 28 S	FEBEX Block 25 W	Rokle Block 14 NW	IBECO Block 11 S	MX-80 Block 1 IN
Sq. Pressure (MPa)	20	30	20	20	30
a_w	0.997	0.979	0.978	0.982	0.994
Specific Conductance (µS/cm, 25°C)	63461	59715	60189	50531	18908
I (M)	0.91	0.85	0.82	0.69	0.26
Water type	Na-Ca-Cl	Na-Ca-Cl	Na-Ca-Cl	Na-Ca-Cl	Na-Cl
SI Anhydrite	0.24	0.14	0.15	0.24	-0.15
SI Gypsum	0.39	0.29	0.30	0.40	
SI Celestine	-0.08	0.04	-0.04	0.01	-0.02
SI Barite	1.16	1.26	1.31	--	1.84
SI Calcite	0.98	0.41	0.79	0.01	-0.02
SI Dolomite	1.16	0.67	1.01	-0.20	-0.15
SI Magnesite	0.45	0.53	0.50	0.06	0.14
SI Strontianite	-0.73	-1.08	-0.79	-1.62	-1.28

SI CO_2 (g)	-3.63	-2.87	-3.28	-2.71	-2.79
SI Chalcedony	1.35	-0.12	-0.41	1.33	-0.06
SI Quartz	1.64	0.17	-0.13	1.62	0.22
Greenrust (OH)	--	6.79	--	--	3.23
Lepidrocrocite	--	5.57	--	--	4.45
Jarosite (K)	--	3.26	--	--	0.31
Goethite	--	7.06	--	--	5.94
Maghemite (dis)	--	12.01	--	--	9.76
Magnetite	--	13.69	--	--	10.05
Hematite	--	14.89	--	--	12.65
Ferrihydrite	--	4.01	--	--	2.89
SI Halite	-2.49	-2.59	-2.51	-2.69	-3.54

Table S11. Chemical composition of the pore waters obtained by squeezing at 25 MPa for water vapour saturated FEBEX, IBECO RW C16, and MX-80 bentonites at initial conditions.

Bentonites	**Febex 28.2% w.c.**(*)	**IBECO RW C16 28.9% w.c.** (*)	**MX80 25.6% w.c.** (*)
Volume (mL)	5	1.75	2
pH	7.3	7.8	8.0
E. C. (μS/cm)	21695	13785	22596
I (M)	0.27	0.19	0.33
Water type	Na-Mg-Cl	Na-SO_4-Cl	Na-SO_4
Cl (mg/L)	6600	2800	1100
SO_4^{2-} (mg/L)	2600	4300	9300
Br^- (mg/L)	12	5	< 5
NO_3^- (mg/L)	143	58	1200
Alkalinity (meq/L)	2.06	2.88	n.d.
Si (mg/L)	14	8.5	< 0.8
Na (mg/L)	3200	2400	4900
K (mg/L)	34	43	59
Ca (mg/L)	649	380	278
Mg (mg/L)	591	312	146
Sr (mg/L)	11	4	6.8
Fe (mg/L)	≤ 0.15	< 0.38	< 0.8
Al (mg/L)	0.27	<0.38	< 0.8
B (mg/L)	1.2	1.2	< 0.8
Mn (mg/L)	0.22	0.96	< 0.8
Ba (mg/L)	< 0.15	< 0.38	< 0.8
pCO_2 (bar)	-2.37	-2.70	--

(*)Raw bentonites samples were submitted to a relative humidity of 100% inside a dessicator containing water during at least 3 months prior to squeezing test.

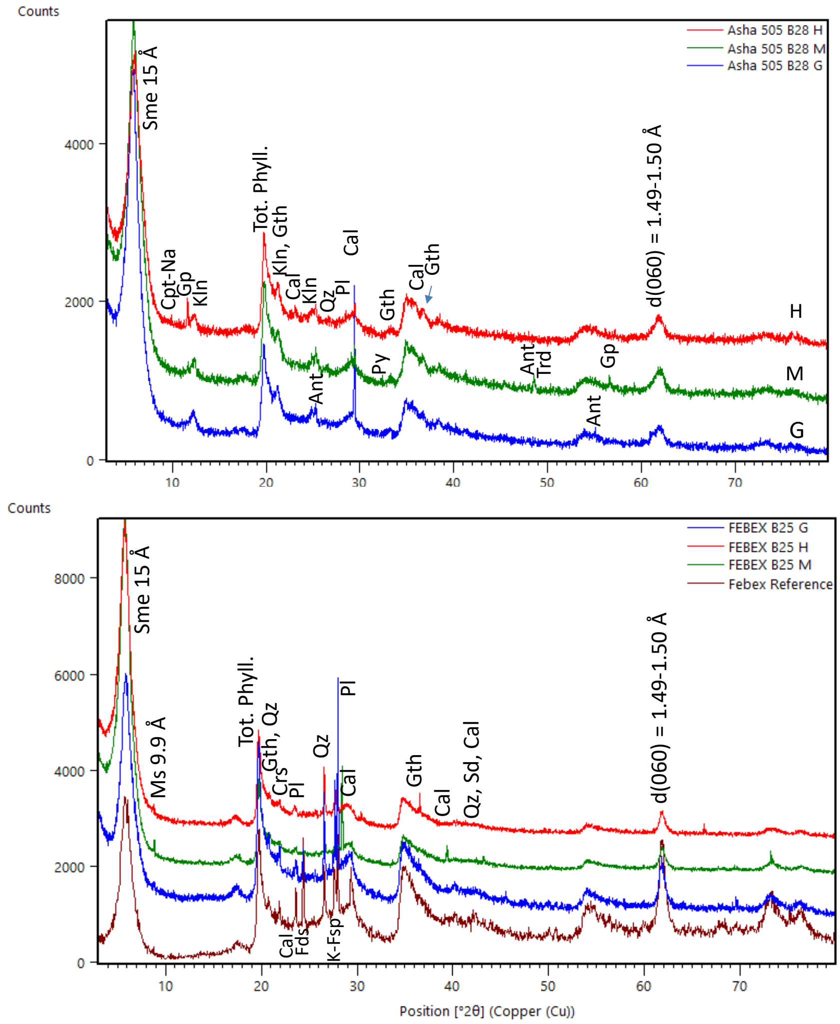
Counts
Asha 505 B28 H
Asha 505 B28 M
Asha 505 B28 G
Sme 15 Å
Cpt-Na
Gp
Kln
Tot. Phyll.
Kln, Gth
Cal
Kln
Qz
Pl
Cal
Gth
Cal
Gth
Py
Ant
Ant
Trd
Gp
Ant
d(060) = 1.49-1.50 Å
H
M
G
Counts
FEBEX B25 G
FEBEX B25 H
FEBEX B25 M
Febex Reference
Sme 15 Å
Ms 9.9 Å
Tot. Phyll.
Gth, Qz
Crs
Pl
Qz
Pl
Cal
Gth
Cal
Qz, Sd, Cal
Cal
Fds
K-Fsp
d(060) = 1.49-1.50 Å
Position [°2θ] (Copper (Cu))

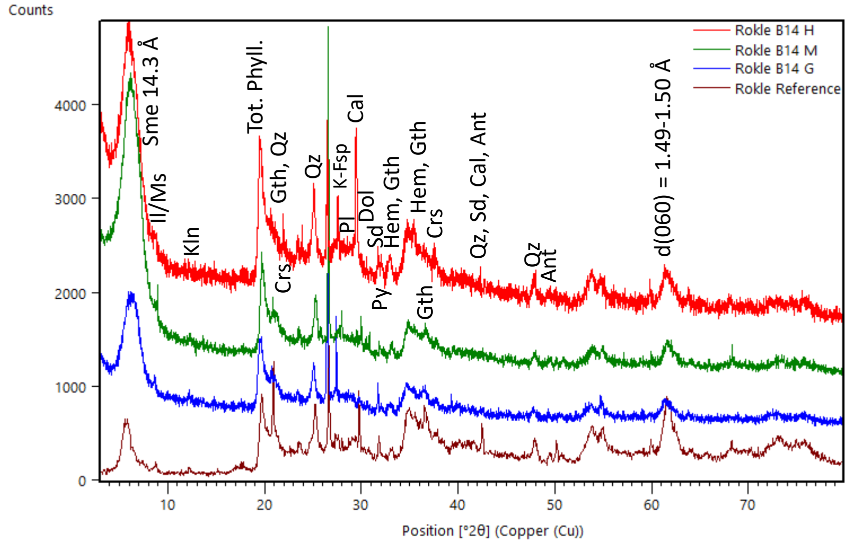
Counts
Rokle B14 H
Rokle B14 M
Rokle B14 G
Rokle Reference
Sme 14.3 Å
Il/Ms
Kln
Tot. Phyll.
Gth, Qz
Crs
Qz
K-Fsp
Pl
Cal
Dol
Sd
Hem, Gth
Hem, Gth
Crs
Py
Gth
Qz, Sd, Cal, Ant
Qz
Ant
d(060) = 1.49-1.50 Å
Position [°2θ] (Copper (Cu))

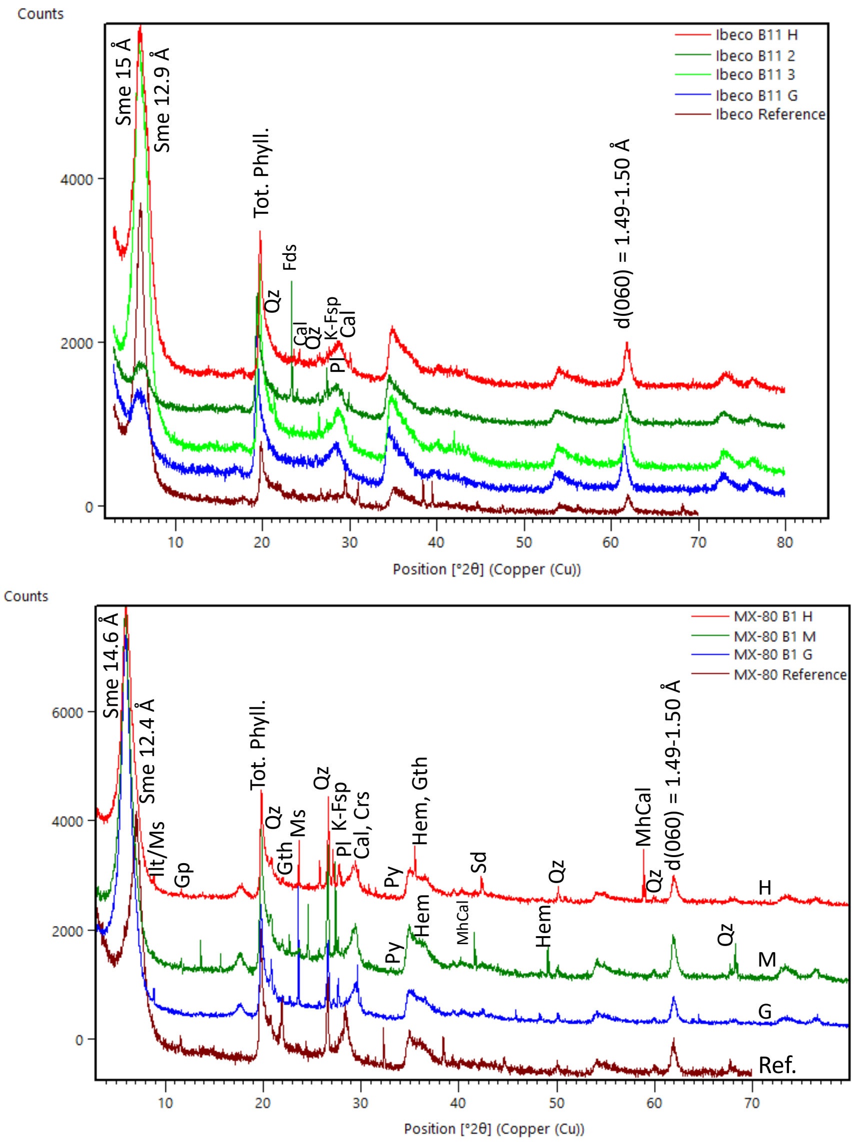

Figure S1. XRD patterns of total fraction samples from ABM5 experiment. Continuation. Symbols according to [13]. Sme: smectite, Ilt/Ms: illite/muscovite, Cpt-Na: Clinoptilolite, Gp: Gypsum, Tot. Phyll: total phyllosilicates, Crs: cristobalite, Cal: calcite, MhCla: monohydrocalcite, Qz: quartz, K-Fsp: potassium feldspar, Pl: Plagioclase, Dol: dolomite, Mgs: magnesite, Gth: goethite, Hem: hematite.

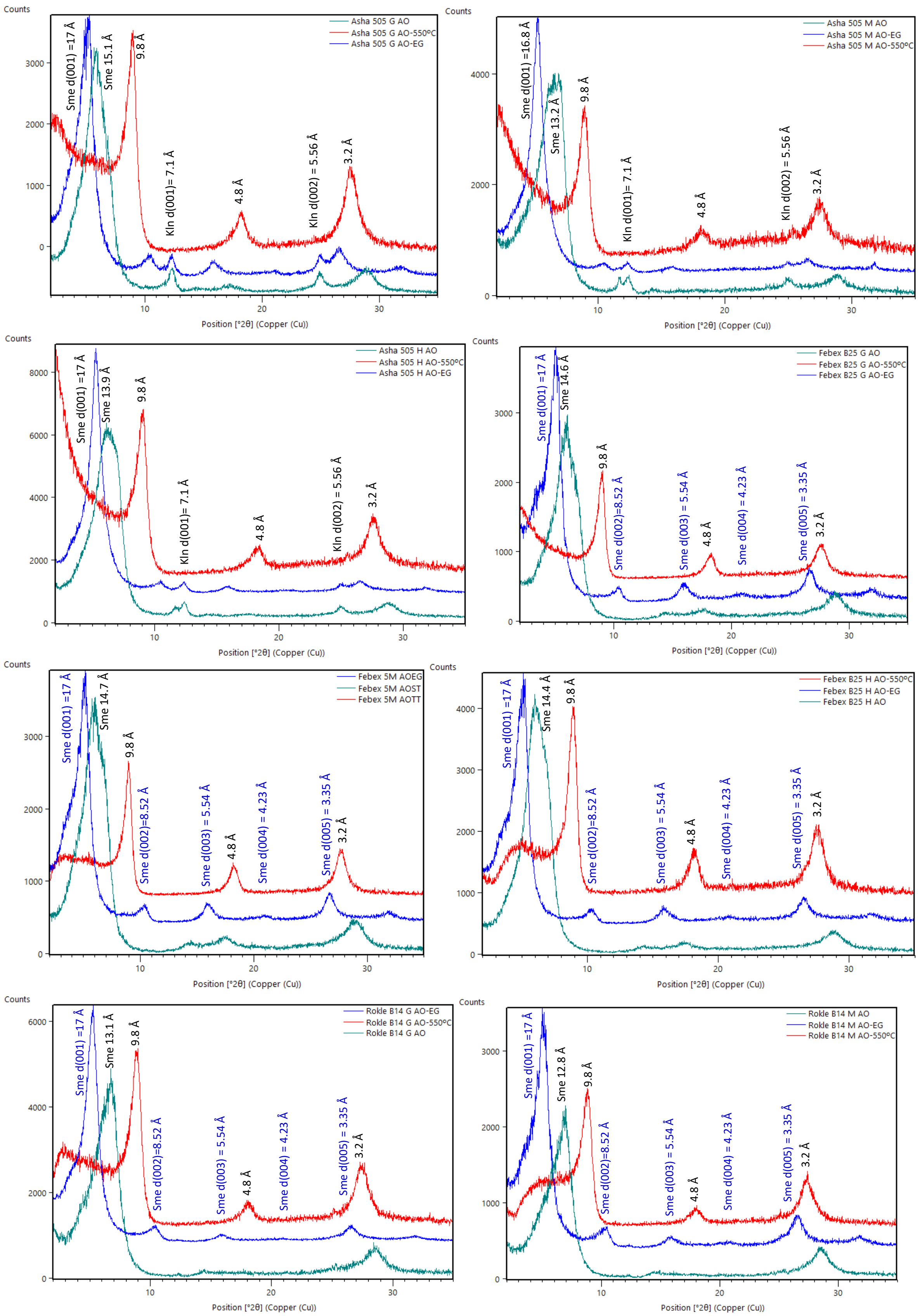
Counts
Asha 505 G AO
Asha 505 G AO-550ºC
Asha 505 G AO-EG
Sme d(001) =17 Å
Sme 15.1 Å
9.8 Å
Kln d(001)= 7.1 Å
4.8 Å
Kln d(002) = 5.56 Å
3.2 Å
Position [°2θ] (Copper (Cu))
Counts
Asha 505 M AO
Asha 505 M AO-EG
Asha 505 M AO-550ºC
Sme d(001) =16.8 Å
Sme 13.2 Å
9.8 Å
Kln d(001)= 7.1 Å
4.8 Å
Kln d(002) = 5.56 Å
3.2 Å
Position [°2θ] (Copper (Cu))
Counts
Asha 505 H AO
Asha 505 H AO-550ºC
Asha 505 H AO-EG
Sme d(001) =17 Å
Sme 13.9 Å
9.8 Å
Kln d(001)= 7.1 Å
4.8 Å
Kln d(002) = 5.56 Å
3.2 Å
Position [°2θ] (Copper (Cu))
Counts
Febex B25 G AO
Febex B25 G AO-550ºC
Febex B25 G AO-EG
Sme d(001) =17 Å
Sme 14.6 Å
9.8 Å
Sme d(002)=8.52 Å
Sme d(003) = 5.54 Å
4.8 Å
Sme d(004) = 4.23 Å
Sme d(005) = 3.35 Å
3.2 Å
Position [°2θ] (Copper (Cu))
Counts
Febex 5M AOEG
Febex 5M AOST
Febex 5M AOTT
Sme d(001) =17 Å
Sme 14.7 Å
9.8 Å
Sme d(002)=8.52 Å
Sme d(003) = 5.54 Å
4.8 Å
Sme d(004) = 4.23 Å
Sme d(005) = 3.35 Å
3.2 Å
Position [°2θ] (Copper (Cu))
Counts
Febex B25 H AO-550ºC
Febex B25 H AO-EG
Febex B25 H AO
Sme d(001) =17 Å
Sme 14.4 Å
9.8 Å
Sme d(002)=8.52 Å
Sme d(003) = 5.54 Å
4.8 Å
Sme d(004) = 4.23 Å
Sme d(005) = 3.35 Å
3.2 Å
Position [°2θ] (Copper (Cu))
Counts
Rokle B14 G AO-EG
Rokle B14 G AO-550ºC
Rokle B14 G AO
Sme d(001) =17 Å
Sme 13.1 Å
9.8 Å
Sme d(002)=8.52 Å
Sme d(003) = 5.54 Å
4.8 Å
Sme d(004) = 4.23 Å
Sme d(005) = 3.35 Å
3.2 Å
Position [°2θ] (Copper (Cu))
Counts
Rokle B14 M AO
Rokle B14 M AO-EG
Rokle B14 M AO-550ºC
Sme d(001) =17 Å
Sme 12.8 Å
9.8 Å
Sme d(002)=8.52 Å
Sme d(003) = 5.54 Å
4.8 Å
Sme d(004) = 4.23 Å
Sme d(005) = 3.35 Å
3.2 Å
Position [°2θ] (Copper (Cu))

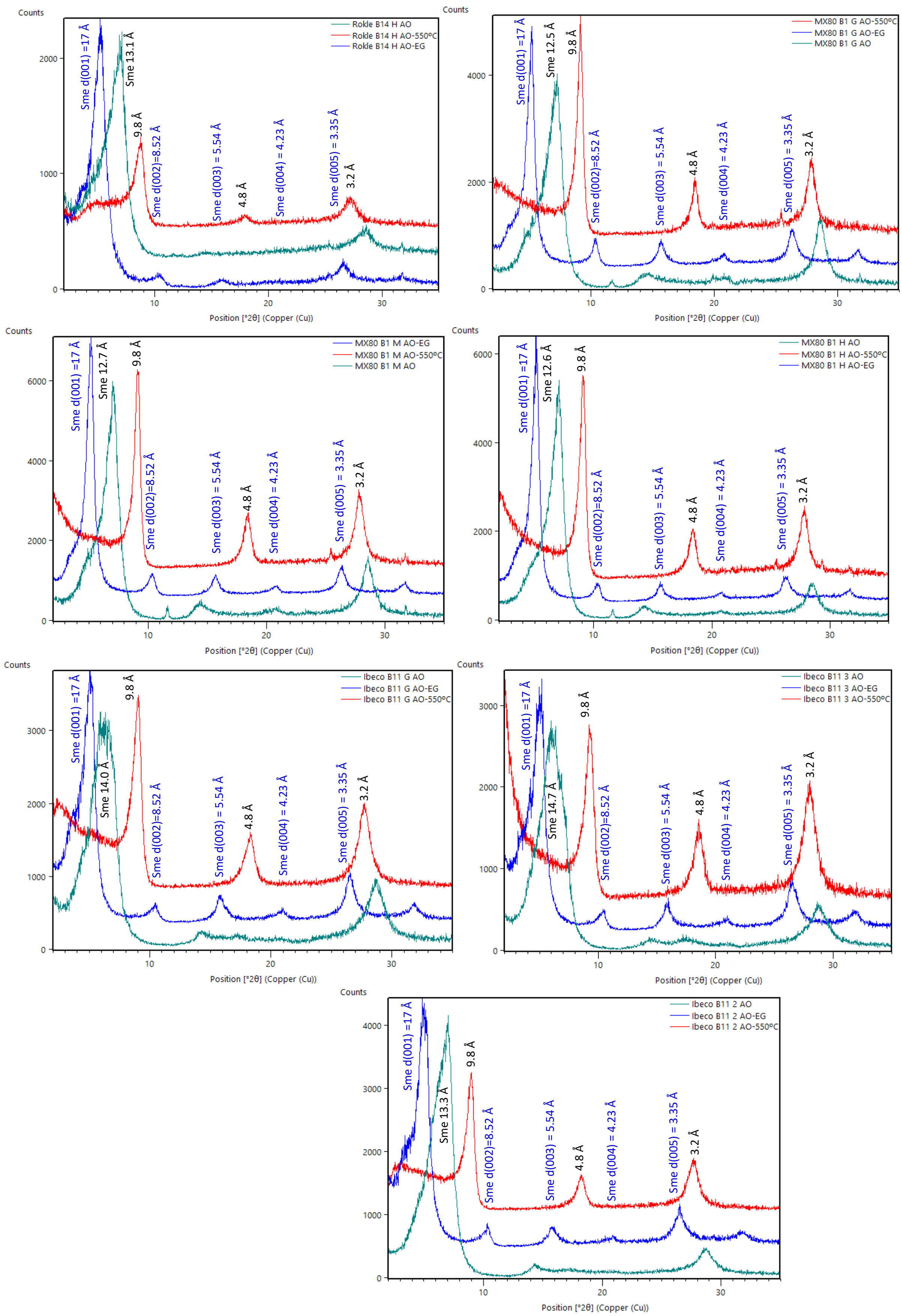

Figure S2. XRD patterns of oriented aggregate samples from ABM5 experiment (normal and after ethylene glycol and heating at 550 °C treatments).

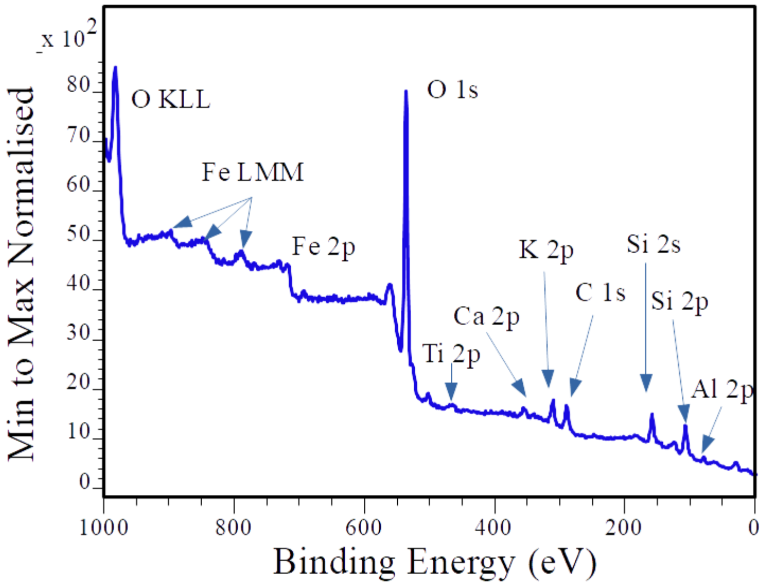

Figure S3. Wide scan XPS spectrum recorded from sample Rokle 4H at heater contact.

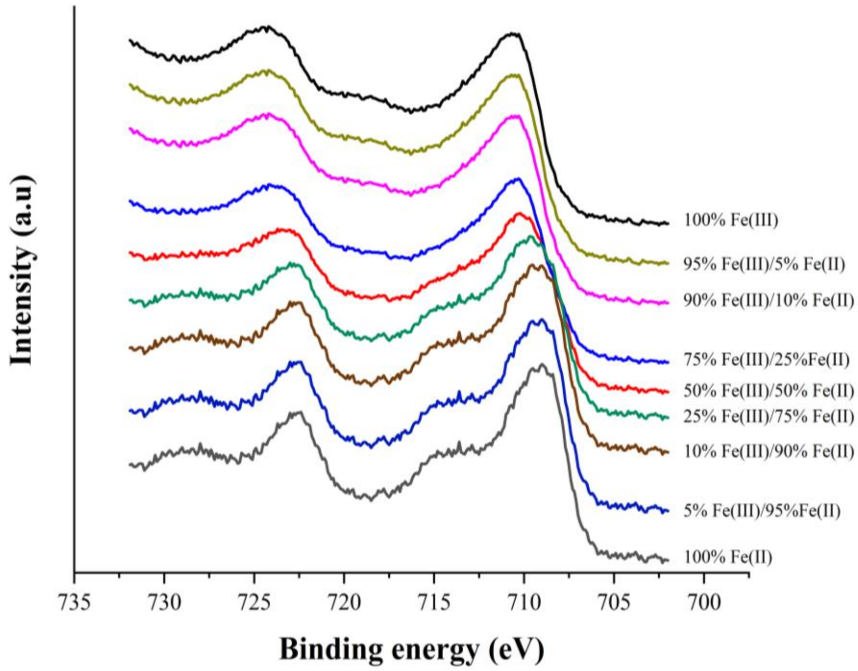

Figure S4. Fe 2p XPS spectra recorded from samples containing different concentrations of Fe(III) and Fe(II) standard compounds.

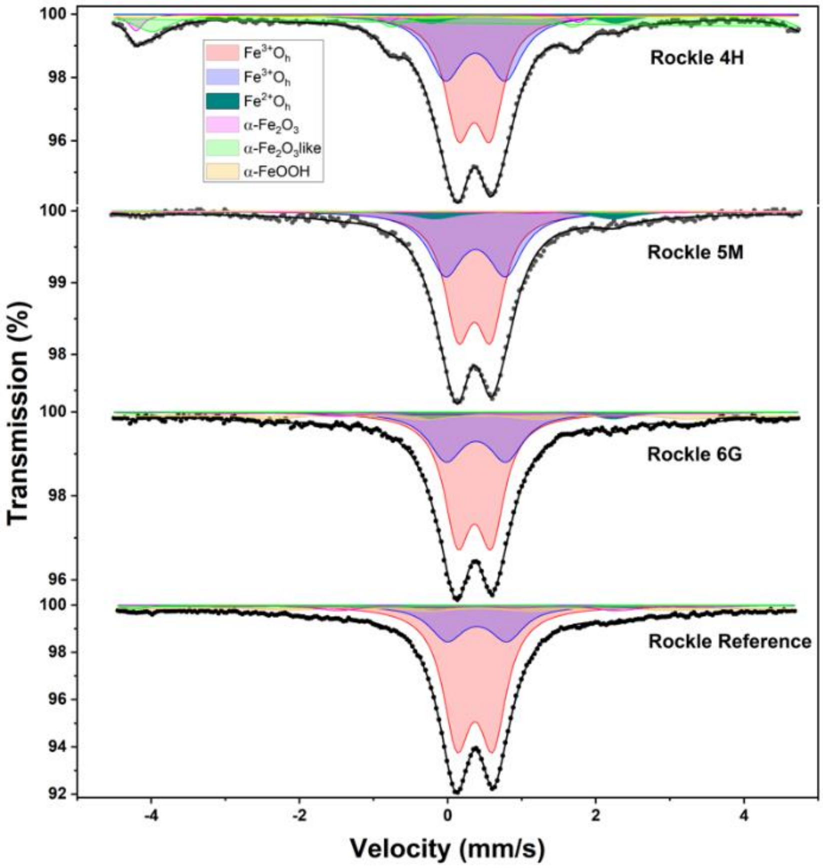

Figure S5. Room temperature Mössbauer spectra recorded in a narrow range of velocities for Rokle samples: reference, 4H: close to heater interface, 5M: middle, and 6G: close to granite interface, i.e., at 1.67 cm, 5.00 cm and 8.33 cm from heater contact, respectively.

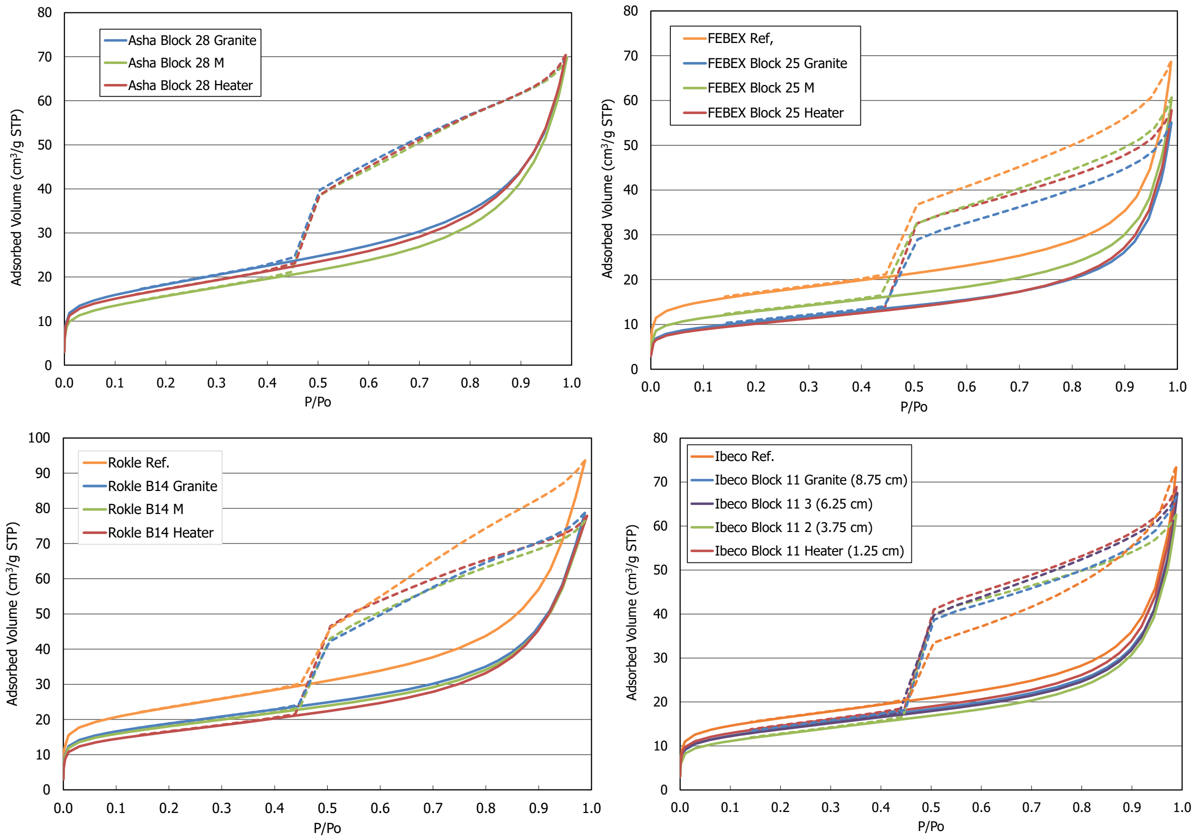

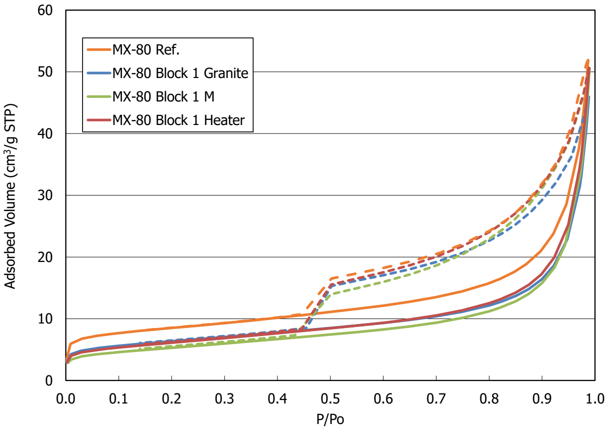

Figure S6. N_2 adsorption/desorption isotherms from reference and retrieved ABM5 samples.

References

1. Slaughter M.; Earley, J. W. Mineralogy and geological significance of the Mowry bentonites, Wyoming. 1965. New York: Geological Society of America. Geological Society of America Special Paper 83.
2. Christidis, G.; Scott, P. W.; Marcopoulos, T. Origin of the bentonite deposits of Eastern Milos, Aegean, Greece: Geological, Mineralogical and Geochemical Evidence. *Clays and Clay Minerals* **1995**, *43*, 63 – 77.
3. Konta, J. Textural variation and composition of bentonite derived from basaltic ash. *Clays and Clay Minerals* **1986**, *34*, 257–265.
4. Přikryl, R.; Woller, F. Going underground: A new market for Czech bentonite in nuclear waste disposal. *Industrial Minerals* **2002**, *415*, 72–77.
5. Huertas, F.; Farina, P.; Farias, J.; Garcia-Sineriz, J.L.; Villar, A.M.; Fernandez, A.M.; Martin, P.L.; Elorza, F.J.; Gens, A.; Sanchez, M.; Lloret, A.; Samper, J.; Martinez, M.A. FEBEX Project. Full-scale Engineered Barriers Experiment for a Deep Geological Repository for High Level Radioactive Waste in Crystalline Host Rock. Updated Final Report 1994-2004. Technical Publication ENRESA 5-0/2006. 2006, pp. 590 (Madrid).
6. Fernandez, A.M.; Baeyens, B.; Bradbury, M.; Rivas, P. Analysis of the pore water chemical composition of a Spanish compacted bentonite used in an engineered barrier. *Physics and Chemistry of the Earth* **2004**, *29*, 105–118.
7. Shah, N. R. Indian bentonite: focus on the Kutch region. *Industrial Minerals* **1997**, *359*, 43–47.
8. Madejová, J., Komadel, P. Information available from infrared spectra of the fine fractions of bentonites. In: The application of vibrational spectroscopy to Clay Minerals and Layered Double Hydroxides. CMS workshop lectures (Kloprogge Eds.), 2005, 66-98. The Clay Minerals Society.
9. Madejová, J., Komadel, P. Baseline studies of the Clay Minerals Society Source Clays: Infrared methods. *Clays and Clay Minerals* **2001**, 49, 410-432.
10. Madejová, J. FTIR techniques in clay mineral studies. *Vibrational Spectroscopy* **2003**, 31, 1-10.
11. Farmer, V.C. The infrared spectra of minerals. Mineralogical Society Monograph 4, 1974, 539 pp. Mineralogical Society, London.
12. Svensson, D.; Sandén, T.; Olsson, S.; Dueck, A.; Eriksson, S.; Jägerwall, S.; Hansen, S. Alternative buffer material Status of the ongoing laboratory investigation of reference materials and test package 1. SKB TR-11-06; Svensk Kärnbränslehantering AB: Stockholm, Sweden, 2011, 146 pp.
13. War, L. IMA–CNMNC approved mineral symbols. *Mineralogical Magazine* **2021**, 85, 291–320.